UNIVERSITY OF
CAMBRIDGE

Encoding Yang-Mills Theory for Quantum Computation

– Part III Essay –

Eliza Somerville

Supervised by Professor Matthew Wingate

8 May 2025

1 Introduction

Our current understanding of the Standard Model of elementary particle physics relies crucially on our understanding of the gauge theory known as Yang-Mills theory. This is, at heart, an interacting theory of spin-1 fields. It is a non-Abelian gauge theory based on a compact Lie group, usually taken to be the special unitary group SU(n). Yang-Mills theories arise in the Standard Model in the theory of the electroweak force, which is based on the gauge group U(1) $\times$ SU(2), and in quantum chromodynamics (QCD), which is the theory of the strong force and is based on the gauge group SU(3).

There remain several open problems in the study of Yang-Mills theory. In particular, there is currently no proof of the mass-gap conjecture, which posits that the lowest excitations of a pure Yang-Mills theory have a finite mass gap with respect to the vacuum. This means that the theory remains an area of active research. However, the study of Yang-Mills theory is complicated by the running of its coupling constant, which means that the theory is strongly coupled at low energies, and thus cannot be treated perturbatively. In this strong-coupling regime, one of the most effective methods of studying the theory is to simulate it numerically. In order to put the theory on a computer, it must be discretised to obtain a *lattice gauge theory*.

To date, most simulations in lattice gauge theory have been performed on classical computers, usually using Markov chain Monte Carlo methods. However, classical simulations can often be inefficient, and for many systems they suffer a *sign problem* which renders the computations intractable. In recent years, there have been major advances in the development of hardware for quantum computation, and this has sparked research into whether near- or distant-future quantum computers could be used to solve problems in quantum field theory which cannot be tackled on classical computers. For digital quantum computers consisting of registers of qubits, an important first issue is how to approximate or 'encode' the infinite-dimensional Hilbert space of the quantum field theory using a finite-dimensional Hilbert space spanned by registers of qubits. This essay focuses on this encoding problem in the case of SU(2) Yang-Mills theory.

1.1 Lattice Gauge Theory

Calculations in quantum field theory can be very challenging, and are often impossible to perform analytically. This means it has been necessary to develop ways of simulating quantum field theories on computers in order to obtain numerical results. However, finding a way of accurately representing such a theory on a computer is itself a difficult task. A quantum field theory has an infinite number of degrees of freedom, and in order to perform simulations we need to replace this original, continuous theory with a new theory that has only a finite number of degrees of freedom. One of the most successful such theories is *lattice gauge theory*, the foundations of which were laid by Kenneth G. Wilson in 1974 [1].

A lattice gauge theory is obtained by discretising a quantum field theory, so that it consists of a large number of *sites*, which we label by n. We will consider hypercubic lattices of total size L in each direction, with sites spaced a distance a apart. The sites are connected by *links*, which we label by ℓ, and the basic variables of the theory are the *link variables* U_ℓ, which will be defined in detail in Section 2. The smallest closed loop of links on the lattice consists of a square formed of four links. Such a loop is known as a *plaquette* and will be denoted by p. Plaquettes form the fundamental building block for defining the field strength of the gauge field on the lattice. These basic components of a lattice gauge theory are illustrated in Figure 1.1.

This discretisation procedure allows the theory to be encoded on a computer, but it also acts to regularise any divergences in the theory. Ultraviolet divergences are regularised by the UV cutoff $\Lambda \sim 1/a$ set by the lattice spacing, while infrared divergences are regularised by the IR cutoff $\sim 1/L$ set

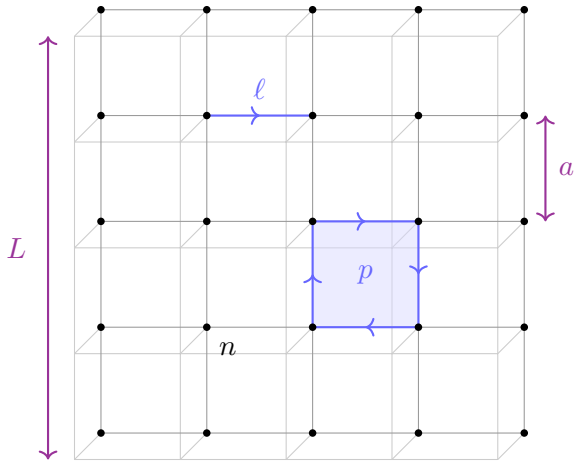

Figure 1.1: A typical lattice configuration showing the basic quantities involved in a lattice gauge theory, including sites n, links ℓ, and plaquettes p. The lattice spacing is a, and the total size of the lattice is L. (Note that the lattice should extend a distance L in all directions; this is not shown in the third direction here to maintain clarity.)

by the lattice size. This means that lattice gauge theories are free from divergences, and are well-defined outside of perturbation theory even at strong coupling. In the double limit $a \to 0, L \to \infty$, the lattice gauge theory should reproduce the behaviour of the original continuum theory [2].

As laid out in [3], there are two main ways in which one can go about discretising a quantum field theory:

- **Euclidean lattice gauge theory** involves discretising both space and time. This is generally done by working with a Euclidean spacetime, which is replaced by a four-dimensional lattice that preserves some discrete subgroup of SO(4). The advantage of this approach is that it preserves some remnant of Lorentz invariance. However, a significant disadvantage of this approach is that the structure of quantum mechanics is lost, and we can no longer work with a Hilbert space. This is the approach most commonly used in simulations on classical computers, such as those performed via the Monte Carlo methods described below.

- **Hamiltonian lattice gauge theory** involves discretising space, but leaving time as a continuous variable. For example, space could be replaced with a cubic, three-dimensional lattice. An advantage of this method is that the structure of quantum mechanics is preserved, and we can discuss states in a Hilbert space and the way they evolve continuously with time. The main disadvantage is that Lorentz invariance has been completely broken, and we must merely hope that it emerges at low energies. This approach is more suited to simulating field theories on quantum computers, and is the approach we will focus on here; in particular, we introduce the Hamiltonian formulation of Yang-Mills theory in Section 3.

1.2 Classical Simulation Methods

Before discussing some of the attempts to implement SU(2) Yang-Mills theory on quantum computers, it is useful to consider how the problem has been tackled on classical computers, and how quantum computers could address some of the problems associated with classical devices.

Monte Carlo Methods

The most common method of simulating quantised Yang-Mills theory on classical computers is through the use of Monte Carlo simulations. One of the first simulations of four-dimensional SU(2) lattice gauge theory was described in [4], in which simulations were performed in the magnetic basis on a lattice with up to 10^4 sites using Monte Carlo techniques. More precisely, a *heat bath* algorithm was used, in which the system was treated by simulating an ensemble in equilibrium at temperature $T = 1/\beta$. Starting in some initial configuration, a heat bath was successively touched to each link variable, so that each U_ℓ was replaced with a new element U'_ℓ chosen randomly from the entire group with probability density proportional to the Boltzmann factor,

$$dP(U'_\ell) \sim \exp[-\beta S(U'_\ell)]\, dU'_\ell, \tag{1.1}$$

where $S(U'_\ell)$ is the action evaluated with the given link having value U'_ℓ and all other links fixed at their previous values, and dU'_ℓ is the Haar measure on the group. In each iteration, this procedure is applied to every link in the lattice. Of all possible Monte Carlo algorithms that vary only a single spin at a time, this method leads to equilibrium in the lowest number of iterations. The results of these simulations provided key evidence for the coexistence of confinement and asymptotic freedom for quantised non-Abelian gauge fields. The algorithm was further refined in [5] in order to obtain a higher acceptance rate for each configuration generated in the Monte Carlo process and thus accelerate the equilibration rate.

One major downside of using Monte Carlo methods to perform numerical simulations of quantum systems is the so-called *sign problem*. This occurs in systems with complex integrands, and essentially means that it is difficult or impractical to sample configurations of the system because the integrand oscillates or has large cancellations between positive and negative values. As a result, the Monte Carlo sampling process cannot efficiently approximate the quantities of interest. While pure gauge Yang-Mills theory in imaginary time does not suffer the sign problem, the problem does arise when fermions are included. The sign problem also means that the real-time dynamics of the theory cannot be accessed using Monte Carlo methods. It is therefore important to develop alternative simulation methods that do not suffer this sign problem.

Tensor Network Methods

One sign-problem-free way of classically simulating quantised Yang-Mills theory for certain lower-dimensional systems is provided by tensor network methods. Tensor network states are a particular representation of quantum many-body states, based on the state's entanglement structure. To illustrate how this works, consider a set of N interacting quantum systems. Let $\{|i_k\rangle\}$ for $i_k = 1, \ldots, d$ denote a basis for the d-dimensional Hilbert space of the quantum system at site k. Then a generic quantum state $|\psi\rangle$ of the whole system can be expressed as a linear combination of all of these basis states,

$$|\psi\rangle = \sum_{i_1,\ldots,i_N=1}^{d} C_{i_1\ldots i_N}\, |i_1\rangle \otimes |i_2\rangle \otimes \cdots \otimes |i_N\rangle\,. \tag{1.2}$$

The tensor $C_{i_1\ldots i_N}$ that provides the coefficients for the many-body basis states has an exponentially large number of complex entries d^N, and thus cannot be stored efficiently on a classical computer.

The basic idea of tensor network methods is to decompose the tensor $C_{i_1\ldots i_N}$ into a network of smaller tensors. A simple example of a family of one-dimensional tensor network states are *matrix product states* (MPS) which parameterise the coefficients of the state as a product of matrices,

$$|\psi\rangle = \sum_{i_1,\ldots,i_N=1}^{d} \mathrm{Tr}\Big(A_1^{i_1} A_2^{i_2} \cdots A_N^{i_N}\Big)\, |i_1\rangle \otimes |i_2\rangle \otimes \cdots \otimes |i_N\rangle\,, \tag{1.3}$$

where $A_k^{i_k}$ are complex matrices of size $D \times D$. This parameter D is called the *bond dimension* of the MPS. In this case, NdD^2 complex numbers must be stored, so provided that D does not grow exponentially with N, the representation is efficient and allows the exponential scaling in the system size to be overcome on a classical computer. For many physically relevant systems, D only shows a polynomial dependence on N, so that the tensor network method provides an effective way of classically simulating these systems [6].

There has already been some success in applying tensor network methods to simulations of Yang-Mills theory in lower dimensions. For example, [7] presents the tensor network simulation of (2+1)-dimensional SU(2) Yang-Mills theory with flavourless fermionic matter. The results confirm that tensor network methods provide a reliable approach to addressing certain systems affected by the sign problem.

One may therefore wonder if quantum computing is really necessary to perform the desired simulations of lattice gauge theories, or if tensor network methods on classical computers may in fact prove to be sufficient for computing the quantities of interest. But there is one major drawback of the tensor network approach: it relies crucially on the fact that most physically-relevant states only carry little entanglement, and thus can be described with tensors of moderate size. However, there are certain situations in which the amount of entanglement is too large to permit an efficient tensor network description.Furthermore, even in situations in which an efficient tensor network description is possible, the computational cost of tensor network algorithms may render the calculation infeasible in practice. At present, tensor network methods have only been applied to non-Abelian gauge theories in (2+1) dimensions, and many algorithmic advances are required in order to extend the method to the (3+1)-dimensional case [6].

Faced with these limitations on classical computations, it is reasonable to ask whether quantum computers may provide a way of overcoming the classical difficulties, and solving important problems in lattice gauge theories in regimes where classical methods fail. We now turn to this approach, beginning by providing a brief introduction to the field of quantum computation.

1.3 Quantum Computation

Quantum computers are devices designed to take advantage of quantum-mechanical phenomena to perform computations more efficiently. In classical computers, the basic unit of information is a *bit*, which can take definite binary values of 0 or 1. In contrast, the basic unit of a quantum computer is a *qubit*, which is a quantum system described by a two-dimensional Hilbert space with the basis states $\{|0\rangle, |1\rangle\}$. The laws of quantum mechanics allow this system to exist in a superposition of the two basis states, so that a general single-qubit state $|\psi\rangle$ can be described as a linear combination

$$|\psi\rangle = \alpha\,|0\rangle + \beta\,|1\rangle\,, \qquad |0\rangle = \begin{pmatrix}1\\0\end{pmatrix}, \quad |1\rangle = \begin{pmatrix}0\\1\end{pmatrix}, \tag{1.4}$$

where α and β are complex numbers satisfying the normalisation condition $|\alpha|^2 + |\beta|^2 = 1$. The basis $\{|0\rangle, |1\rangle\}$ is referred to as the *computational basis*. When performing a projective measurement of the qubit in this basis, the probability of measuring the qubit to be in state $|0\rangle$ is $|\alpha|^2$, while the probability of measuring it to be in state $|1\rangle$ is $|\beta|^2$. The capacity of qubits to exist in superpositions of the basis states means that a system of N qubits can be in a superposition of all 2^N possible basis states, which allows an exponentially large Hilbert space to be encoded efficiently [6].

Quantum Circuits

Calculations made using quantum computers are most commonly described using a quantum circuit. The process of executing a quantum circuit consists of three stages:

1. All N qubits are initialised in state $|0\rangle$.

2. Quantum gates, represented by unitary operators, are applied to some or all of the qubits.

3. Measurements of some or all of the qubits are made in the computational basis.

This process can be conveniently visualised in a quantum circuit diagram, in which time flows from left to right. Each single line represents a qubit, while each double line represents a classical bit. The symbols on the wires represent operations performed on the qubits, such as gate operations or projective measurements [6]. In such circuits, operations may be performed on qubits by applying quantum gates, which represent unitary transformations. These gates may be applied to a single qubit, or to multiple qubits simultaneously. The most common single-qubit quantum gates are

Hadamard 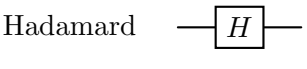 $\frac{1}{\sqrt{2}}\begin{pmatrix}1 & 1\\ 1 & -1\end{pmatrix}$

Pauli-X 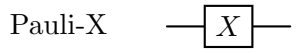 $\begin{pmatrix}0 & 1\\ 1 & 0\end{pmatrix}$

Pauli-Y 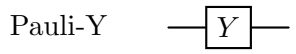 $\begin{pmatrix}0 & -i\\ i & 0\end{pmatrix}$

Pauli-Z 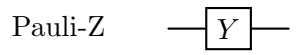 $\begin{pmatrix}1 & 0\\ 0 & -1\end{pmatrix}$.

We can in fact represent any single-qubit gate as a parametric rotation by an angle θ about an axis $\hat{\mathbf{n}}$,

$$R_{\mathbf{n}}(\theta) = \exp(-i\theta\hat{\mathbf{n}}\cdot\boldsymbol{\sigma}/2), \tag{1.5}$$

where $\boldsymbol{\sigma} = (\sigma^1, \sigma^2, \sigma^3)$ is a vector of Pauli sigma matrices.

A commonly-used two-qubit gate is the controlled-NOT gate,

CNOT 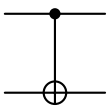 $\begin{pmatrix}1 & 0 & 0 & 0\\ 0 & 1 & 0 & 0\\ 0 & 0 & 0 & 1\\ 0 & 0 & 1 & 0\end{pmatrix}$,

which is applied to a two-qubit state $|\psi_1\rangle \otimes |\psi_2\rangle$, represented as a four-dimensional column vector. In the case shown above, the qubit in the top wire is the control, represented by $\bullet$, while the qubit in the bottom wire is the target, represented by $\oplus$. The position of the control and the target can be interchanged by applying Hadamard gates to both of the qubits before and after the CNOT gate is applied:

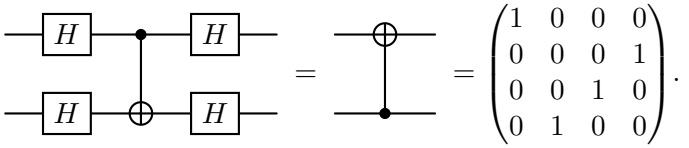 $= \begin{pmatrix}1 & 0 & 0 & 0\\ 0 & 0 & 0 & 1\\ 0 & 0 & 1 & 0\\ 0 & 1 & 0 & 0\end{pmatrix}$.

It can in fact be shown that the set of all single-qubit quantum gates, along with the CNOT gate, form a universal set of quantum gates [8]. This means that all unitary operations on arbitrarily many bits can be expressed as compositions of these elementary gates.

Trotterisation

In quantum mechanics, the time evolution operator of a system with Hamiltonian H is given by $U(t) = e^{-iHt}$. Since this operator is exponentially large, it is usually very computationally intensive to compute exactly. This means it is useful to break the Hamiltonian down into a sum of terms, each of which acts on a much smaller subsystem and can be approximated in a straightforward manner using quantum circuits.

For simplicity, let us consider the example where H can be written as a sum of two terms, $H = H_A + H_B$. If H_A and H_B commute, then we can simply perform simulations of systems corresponding to each term separately, and then determine the time evolution of the whole system using the formula $e^{-iHt} = e^{-iH_At}e^{-iH_Bt}$.

However, additional complexity arises when these two terms do not commute with each other, so that $[H_A, H_B] \neq 0$. In this case, it is no longer the case that $e^{-iHt} = e^{-iH_At}e^{-iH_Bt}$. To determine the time evolution operator of the whole system, we instead resort to the first-order *Trotter formula*, which states that

$$e^{-i(H_A+H_B)t} \approx \left(e^{-iH_At/n}e^{-iH_Bt/n}\right)^n \tag{1.6}$$

for large n, where n is the *number of Trotter steps*. This means we can continue to split up our Hamiltonian for ease of computation, and then at the end approximate the whole time-evolution operator using the Trotter formula, provided we use an appropriately large number of Trotter steps [9]. This will be relevant when we come to consider experimental realisations of the quantum simulation of Yang-Mills theory in Section 5.

Benefits and Drawbacks of Quantum Computation

There is much interest in the development of quantum computers because they offer the possibility of performing certain calculations substantially more efficiently than classical computers by making use of quantum parallelism, which is based on the fact that qubits exist in superpositions of the basis states. Quantum computers are particularly well-suited to simulating many-body quantum systems, which require exponentially large classical resources, but can be simulated *natively* on quantum computers using unitary operations. Indeed, one of the seminal works in the field of quantum computing was a paper by Feynman published in 1982, which proposed that classical computers would never be able to efficiently simulate the evolution of a quantum system, and suggested that quantum-mechanical phenomena would need to be incorporated into computer hardware [10].

The major obstacle to the use of quantum computers for most practical purposes is the considerable level of noise suffered by current quantum devices. This can result in significant errors being present in the final results of quantum computations. These may stem from gate errors, measurement errors, or thermal relaxation errors. We are currently in the era of Noisy Intermediate-Scale Quantum (NISQ) devices, in which digital quantum computers have $\mathcal{O}(10-100)$ noisy qubits. These NISQ devices are already able to outperform classical computers in certain cases, but the noise means that there is a limit to the depth of quantum circuits that can be faithfully executed. This means that the development of error mitigation and error correction techniques remains the main challenge currently facing quantum computing, and will be essential for achieving quantum advantage for large-scale problems relevant to physics [6].

1.4 Outline of the Essay

We begin in Section 2 by providing a brief overview of Yang-Mills theory and introducing its Hamiltonian formulation. In Section 3, we simultaneously quantise the theory and put it on a lattice to obtain

the Kogut-Susskind Hamiltonian. In Section 4, we introduce the bases which are most often used to simulate Yang-Mills theory, including the electric and magnetic bases, and we also discuss some common truncation schemes. In Section 5, we discuss some recent attempts to simulate SU(2) Yang-Mills theory. Finally, in Section 6, we present some conclusions and discuss possible avenues for future research.

2 Yang-Mills Theory

Yang-Mills theory is one of the most important frameworks in modern theoretical physics because it provides the foundation for our understanding of fundamental forces. In essence, it is a generalisation of Maxwell's theory of electromagnetism to systems with more complex gauge symmetries, particularly those with SU(N) gauge groups. In this section we provide a brief introduction to the mathematical framework underlying Yang-Mills theory, beginning by discussing Lie groups and Lie algebras. This will allow us to build up to introducing the Yang-Mills Lagrangian and Hamiltonian at the end of the section.

2.1 Lie Groups and Lie Algebras

To properly discuss SU(2) Yang-Mills theory, we must begin by introducing the concept of a Lie group and its associated Lie algebra. The following discussion is based on [2, 11].

We focus on continuously generated groups, which contain elements arbitrarily close to the identity. In this case, an infinitesimal group element g can be written as

$$g(\alpha) = 1 + i\alpha^a T^a + \mathcal{O}(\alpha^2), \tag{2.1}$$

where the α^a are the infinitesimal group parameters, and the T^a are Hermitian operators called the *generators* of the group. A group with this structure is called a *Lie group*.

Since the set of generators T^a must span the space of infinitesimal group transformations, the commutator of two generators must itself be a linear combination of generators. This implies that

$$[T^a, T^b] = if^{abc}T^c, \tag{2.2}$$

for some numbers f^{abc} called *structure constants*. The vector space spanned by the generators T^a, with the added operation of commutation, is called the *Lie algebra* of the Lie group. For our purposes, we will assume that we are working with a Lie algebra that has a finite number of generators. Such Lie algebras are called *compact*. We normalise the generators of the defining representation so that

$$\mathrm{Tr}\Big(T^a T^b\Big) = \frac{1}{2}\delta_{ab}. \tag{2.3}$$

The Lie Group SU(2)

In this work, we focus on the Lie group SU(2). This is the group of 2×2 special unitary matrices, that is, complex-valued 2×2 matrices U such that $U^\dagger U = \mathbb{1}$. The generators of the Lie algebra of SU(2) can be taken to be $T^a = \sigma^a/2$, where σ^a are the Pauli matrices,

$$\sigma^1 = \begin{pmatrix} 0 & 1 \\ 1 & 0 \end{pmatrix}, \qquad \sigma^2 = \begin{pmatrix} 0 & -i \\ i & 0 \end{pmatrix}, \qquad \sigma^3 = \begin{pmatrix} 1 & 0 \\ 0 & -1 \end{pmatrix}. \tag{2.4}$$

For this choice of generators, the structure constants of SU(2) are $f^{abc} = \epsilon^{abc}$. An element $U \in$ SU(2) can be expressed in terms of the Lie algebra generators as

$$U = \exp(i\omega^a T^a), \tag{2.5}$$

for some coefficients ω^a. Geometrically, the matrices U are the generators of spinor rotations in three-dimensional space, and the ω^a are the corresponding angles of rotation [12].

We are interested in gauge theories which have the gauge group SU(2), so it is now time to turn to a discussion of gauge invariance, and properly define what we mean by a gauge theory. For the rest of this section, our presentation will follow that of [2]. We will mainly formulate our statements to be applicable for a general gauge group, specialising to SU(2) only when necessary.

2.2 Gauge Invariance

Consider a physical system whose Lagrangian $\mathcal{L}$ is invariant under a compact Lie group G. Let $\psi(x)$ be a field at position x in representation r of G. The invariance of the Lagrangian under G requires that $\psi(x)$ appears in the Lagrangian in such a way as to be invariant under the transformation

$$\psi(x)^i \mapsto D^r(\Omega(x))^i_j \psi(x)^j, \tag{2.6}$$

for all group-valued functions $\Omega(x) \in G$. The set of all such functions Ω is called the *gauge group* of the theory (although G itself may also occasionally be referred to as the gauge group). The object $D^r(\Omega)^i_j$ is the group element Ω in representation r, which is a $(\dim r \times \dim r)$ matrix.

In order to include a kinetic term in the Lagrangian, we must find a way of including derivatives of the field ψ. To take a such a derivative, the values of the field at two nearby points must be compared according to

$$\lim_{a \to 0} \frac{\psi(x+a) - \psi(x)}{a}. \tag{2.7}$$

However, this object is not gauge covariant, since the two values of ψ may be rotated independently in colour space. So in order to construct a gauge-covariant kinetic term, we need to find a way of comparing the value of ψ at different points. We thus define the *gauge-covariant derivative*,

$$D_\mu \psi(x) = \partial_\mu \psi(x) - i A_\mu(x) \psi(x), \tag{2.8}$$

where $A_\mu : \mathbb{R}^{1,3} \to L(G)$ is the *gauge field*, which may be expanded as $A_\mu = A^a_\mu T^a$. In order for (2.8) to be gauge covariant, it must transform under a gauge transformation in the same way as ψ itself:

$$D_\mu \psi(x)^i \mapsto D^r(\Omega(x))^i_j D_\mu \psi(x)^j. \tag{2.9}$$

This will be the case provided that the gauge field A_μ transforms as

$$A_\mu(x) \mapsto \Omega(x) A_\mu \Omega^{-1}(x) + i \Omega(x) \partial_\mu \Omega^{-1}(x). \tag{2.10}$$

The gauge field A_μ has the mathematical function of a connection, and leads to parallel transport, as we now show.

2.3 Wilson Lines

Once we come to put our gauge theory on a lattice, the gauge field A_μ will no longer be the basic object of the theory. Instead, it will be replaced by an object called a *Wilson line*, which encodes the parallel transport of a particle in the gauge field. It is thus useful to introduce the idea of Wilson lines at this stage.

Consider a point particle in the representation r which is colour-charged; that is, suppose that it has a colour vector of dimension r associated with it. Assume that this particle follows some prescribed

path along the worldline $x^\mu(\tau)$ in the presence of a background connection $A_\mu(x)$. In the absence of external forces, the colour charge $w(x)$ of the particle must satisfy the parallel transport equation,

$$\frac{\mathrm{d}w(x(\tau))}{\mathrm{d}\tau} = i\frac{\mathrm{d}x^\mu(\tau)}{\mathrm{d}\tau}A_\mu(x(\tau))w(x(\tau)). \tag{2.11}$$

Since A_μ is Hermitian, we note that the form of the right-hand side of this equation guarantees that the magnitude of the colour charge w is constant.

If we consider the path P starting at $x_i \equiv x(\tau_i)$ and ending at $x_f \equiv x(\tau_f)$, then the solution to the differential equation (2.11) is of the form

$$w(x_f) = U(x_f, x_i; P)w(x_i) \tag{2.12}$$

for some unitary matrix U which depends on the starting point, the endpoint, and the particular path followed. By integrating (2.11), we obtain

$$\begin{aligned} U(x_f, x_i, P) &= \mathcal{P}\exp\left(i\int_{\tau_i}^{\tau_f}\mathrm{d}\tau\,\frac{\mathrm{d}x^\mu}{\mathrm{d}\tau}A_\mu(x(\tau))\right) \\ &= \mathcal{P}\exp\left(i\int_{x_i}^{x_f}\mathrm{d}x^\mu\,A_\mu(x)\right), \end{aligned} \tag{2.13}$$

where $\mathcal{P}\exp$ indicates a *path-ordered exponential*. This means that in the Taylor expansion of the exponential, any $A_\mu(\tau)$ at earlier times on the path are placed to the right of those at later times. The connection A_μ appearing in this equation may be put in any representation $A_\mu = A_\mu^a T^{ra}$, in which case the resulting object transports charges in representation r. The object $U(x_f, x_i; P)$ is called a *Wilson line*, and on the lattice this, rather than the connection itself, is considered to be the basic object of the theory. From (2.10) and the properties of path-ordering, we find that under a gauge transformation,

$$U(x_f, x_i; P) \mapsto \Omega(x_f)U(x_f, x_i; P)\Omega(x_i)^\dagger. \tag{2.14}$$

This equation shows that the Wilson line only takes a gauge-independent value when it is taken around a closed loop C. We thus deduce that local gauge invariant objects may be constructed by considering parallel transport around an infinitesimal loop.

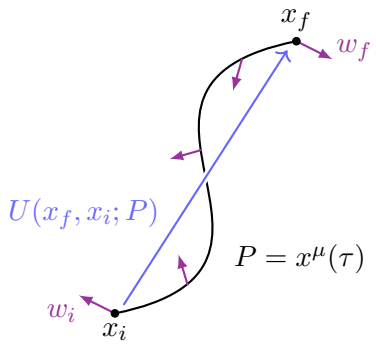

Figure 2.1: When a particle travels along the worldline $P = x^\mu(\tau)$ from x_i to x_f, its colour charge w is transported by the Wilson line $U(x_f, x_i; P)$. Based on a diagram from [2].

2.4 The Yang-Mills Lagrangian

We now aim to write down a locally gauge invariant Lagrangian to describe our theory, using some expression in terms of the gauge field A_μ. As just discussed, local gauge invariant objects may be constructed by considering parallel transport around an infinitesimal loop. We thus consider a very small parallelogram with sides ξ^μ and ζ^ν, which we take to be our closed loop C. In the limit $\xi, \zeta \to 0$, we can write the effect of parallel-transporting the charge w around C as

$$[U(C)w - w] = -iF_{\mu\nu}\xi^\mu\zeta^\nu w, \tag{2.15}$$

for some tensor $F_{\mu\nu}$. By Taylor expanding the path-ordered exponential to second order, we obtain the usual expression for the *field strength tensor*,

$$F_{\mu\nu} = \partial_\mu A_\nu - \partial_\nu A_\mu - i[A_\mu, A_\nu]. \tag{2.16}$$

This object is gauge *covariant*, as according to (2.10) it transforms as

$$F_{\mu\nu}(x) \mapsto \Omega(x)F_{\mu\nu}(x)\Omega(x)^\dagger. \tag{2.17}$$

By the cyclicity of the trace operation, this means that the trace of the field strength tensor is locally gauge *invariant*. We can thus form the locally gauge invariant Lagrangian

$$\mathcal{L}_{\text{YM}} = -\frac{1}{2g^2}\operatorname{Tr} F_{\mu\nu}F^{\mu\nu}, \tag{2.18}$$

where g is a coupling constant. This is the standard form of the *Yang-Mills Lagrangian*.

2.5 The Yang-Mills Hamiltonian

In order to obtain the canonical quantisation of this theory, we must switch from the Lagrangian formulation to the Hamiltonian formulation. To do this, we first find the canonical momenta, which are given by

$$\pi^0 = \frac{\partial\mathcal{L}}{\partial\dot{A}_0} = 0, \tag{2.19}$$

$$\pi^i = \frac{\partial\mathcal{L}}{\partial\dot{A}_i} = -\frac{1}{g^2}F^{0i} \equiv \frac{1}{g^2}E^i, \tag{2.20}$$

where we have defined the *chromo-electric field* $\mathbf{E} = \mathbf{E}^a T^a$. We similarly define the *chromo-magnetic field* $\mathbf{B}$ by $\epsilon_{ijk}B^a_k = F^a_{ij}$.

The canonical Hamiltonian of Yang-Mills theory is therefore

$$\begin{aligned}\mathcal{H}_{\text{YM}} &= \pi^{ia}\dot{A}^a_i - \mathcal{L}_{\text{YM}} \\ &= \frac{1}{2g^2}\Big(E^{ia}E^{ia} + B^{ia}B^{ia} - 2A^a_0(\partial_i E^{ia}) + f_{abc}A^b_i E^{ic})\Big) \\ &= g^2\operatorname{Tr}\boldsymbol{\pi}^2 + \frac{1}{g^2}\operatorname{Tr}\mathbf{B}^2 - \frac{1}{g^2}A^a_0(D_iE^i)^a,\end{aligned} \tag{2.21}$$

where the covariant divergence of the electric field is given by

$$(D_iE^i) \equiv \partial_i E^i - i[A_i, E^i]. \tag{2.22}$$

When working in the Hamiltonian formulation, it is convenient to work in the Weyl gauge, in which $A_0 = 0$. This is an incomplete gauge-fixing condition, since we can still make arbitrary gauge transformations $\Omega(\mathbf{x})$ which are only functions of space. This choice of gauge ensures that the Hamiltonian is gauge invariant. It also means that Gauss' law $\mathcal{D}_i E^i = 0$ is no longer a Hamiltonian equation of motion but instead becomes a supplementary constraint. This is evident in (2.21), where A_0 appears as a Lagrange multiplier enforcing Gauss' law. This means that when $A_0 = 0$ is imposed from the start, Gauss' law must be imposed as a condition on the states of the Hilbert space in the quantised theory. The consequences of this for lattice gauge theory will be discussed further below.

3 The Kogut-Susskind Hamiltonian

Having derived the canonical Hamiltonian of Yang-Mills theory, we now wish to quantise it and put it on a lattice. This procedure was first carried out by Kogut and Susskind [13, 14], and results in the *Kogut-Susskind Hamiltonian*. In this section, we mainly follow the presentation of [2].

3.1 Hamiltonian Formulation of a Lattice Gauge Theory

We begin by introducing the Hamiltonian formulation of a lattice gauge theory. In such a theory, the continuous spatial degrees of freedom are replaced by a discrete set associated with a lattice with spacing a, while time remains a continuous variable. We take the spatial lattice to be hypercubic, with sites labelled by n and links $\ell = \ell(n, e_i)$ joining the adjacent sites n and $n + e_i$, where e_i is a unit vector along the i-th positive direction for $i = 1, \ldots, d$.

Since the primary function of the gauge field A_μ is to transport colour charge, and colour charges reside only on the sites n, the only quantities we need are the Wilson lines $U(n_f, n_i; P)$ joining adjacent sites, and products of these lines. Instead of working with the gauge field A_μ, we will work directly with the Wilson lines $U(n, e_i; P_\ell)$, where the path P_ℓ is the straight line along the link connecting the two adjacent points. This Wilson line may be regarded as a single degree of freedom via the process of coarse graining.

Following [2], we will now simultaneously quantise the theory and put it on a lattice. We will first define the Hilbert space at a single link of the lattice, and then we will place a copy of this Hilbert space on every link of the full lattice to obtain the lattice Hamiltonian.

3.2 Hilbert Space of a Single Link

We start by defining the Hilbert space at a single link of the lattice. We note that in order to fully specify a quantum field theory, we must define both the action and the measure of the path integral. The appropriate measure for lattice gauge theory is known as the *Haar measure* $\mathrm{d}\mathfrak{g}$, which is the unique measure over the group manifold G which satisfies the following properties [3]:

1. Left and and right invariance: For any function $f(\mathfrak{g})$ with $\mathfrak{g} \in G$ and for any $\Omega \in G$,

$$\int \mathrm{d}\mathfrak{g}\, f(\mathfrak{g}) = \int \mathrm{d}\mathfrak{g}\, f(\Omega\mathfrak{g}) = \int \mathrm{d}\mathfrak{g}\, f(\mathfrak{g}\Omega). \tag{3.1}$$

2. Linearity: For any functions $f(\mathfrak{g}), g(\mathfrak{g})$ with $\mathfrak{g} \in G$, and for any scalars α, β,

$$\int \mathrm{d}\mathfrak{g}\, (\alpha f(\mathfrak{g}) + \beta g(\mathfrak{g})) = \alpha \int \mathrm{d}\mathfrak{g}\, f(\mathfrak{g}) + \beta \int \mathrm{d}\mathfrak{g}\, g(\mathfrak{g}). \tag{3.2}$$

3. Normalisation: Denoting the volume of the group manifold G by $|G|$, we have

$$\int \mathrm{d}\mathfrak{g} = |G|. \tag{3.3}$$

The only degree of freedom on link ℓ is the Wilson line $U_\ell \in G$, which we will refer to as the *link variable* (or *link operator* after quantisation). The Hilbert space of a single link is then $L^2(G, \mathrm{d}\mathfrak{g})$, the space of square-integrable functions over the Lie group G with respect to the Haar measure $\mathrm{d}\mathfrak{g}$. One method of describing this space is through the *group element basis*, which are states $|\mathfrak{g}\rangle$ of definite value on SU(2) and may be thought of as position eigenstates. A general state $|\Psi\rangle$ may be expanded in the group element basis as

$$|\Psi\rangle = \int \mathrm{d}\mathfrak{g}\, \Psi(\mathfrak{g})\, |\mathfrak{g}\rangle\,. \tag{3.4}$$

The link $\ell(n, e_i)$ has an orientation inherited from the lattice positive direction $+e_i$. We refer to the oriented start of the link as the *left* side of the link, and the oriented end of the link as the *right* side of the link.

From (2.14), we see that gauge transformations enacted at site n will affect the state of the link via left group composition, while those enacted at $n + e_i$ will affect it via right group composition. We thus define left and right translation operators, which are parameterised by a group element $\mathfrak{g}$ and act on a basis state $|\mathfrak{h}\rangle$ at each link ℓ via left and right group composition as

$$\hat{\Theta}_{L\mathfrak{g}}\, |\mathfrak{h}\rangle = |\mathfrak{g}^{-1}\mathfrak{h}\rangle\,, \quad \hat{\Theta}_{R\mathfrak{g}}\, |\mathfrak{h}\rangle = |\mathfrak{h}\mathfrak{g}^{-1}\rangle\,. \tag{3.5}$$

For a compact Lie group G, these translation operators can always be expressed as

$$\hat{\Theta}_{L\mathfrak{g}} = e^{i\phi^a(\mathfrak{g})\hat{E}^a_L}, \quad \hat{\Theta}_{R\mathfrak{g}} = e^{i\phi^a(\mathfrak{g})\hat{E}^a_R}, \tag{3.6}$$

where $\phi^a(\mathfrak{g})$ is a set of $\dim(G)$ parameters, called normal coordinates, which specify the group element $\mathfrak{g}$, and $\hat{E}_L$ and $\hat{E}_R$ are Hermitian operators. These operators provide two independent Lie algebras of the group, with commutation relations derived from (3.5) and (3.6):

$$\begin{aligned} \left[\hat{E}^a_L, \hat{E}^b_L\right] &= -if^{abc}\hat{E}^c_L \\ \left[\hat{E}^a_R, \hat{E}^b_R\right] &= if^{abc}\hat{E}^c_R \\ \left[\hat{E}^a_L, \hat{E}^b_R\right] &= 0. \end{aligned} \tag{3.7}$$

From representation theory we know that the irreducible representations of compact Lie groups may always be taken to be unitary matrices $D^r_{mm'}$ with dimension $\dim(r) \times \dim(r)$. For SU(2), these are the spin-j representations with $j = 0, 1/2, 1, \ldots$ and dimension $2j + 1$, which we will denote by $D^j_{mm'}(\mathfrak{g})$. We then define the spin-j unitary link operators by

$$\hat{U}^j_{mm'}(\ell) \equiv \int \mathrm{d}\mathfrak{g}_\ell\, D^j_{mm'}(\mathfrak{g}_\ell)\, |\mathfrak{g}_\ell\rangle\, \langle\mathfrak{g}_\ell|\,, \tag{3.8}$$

where ℓ denotes the particular link with which this operator is associated. These operators are all simultaneously diagonal in the group element basis, so they all commute with one another. They may be thought of as position operators.

Under left translation, these link operators transform as

$$\begin{aligned}\hat{\Theta}_{L\mathfrak{g}}\hat{U}^j_{mn}\hat{\Theta}^\dagger_{L\mathfrak{g}} &= \int \mathrm{d}\mathfrak{g}_\ell\, D^j_{mn}(\mathfrak{g}_\ell)\Big(\hat{\Theta}_{L\mathfrak{g}}\,|\mathfrak{g}_\ell\rangle\Big)\Big(\langle\mathfrak{g}_\ell|\,\hat{\Theta}^\dagger_{L\mathfrak{g}}\Big)\\ &= \int \mathrm{d}\mathfrak{g}_\ell\, D^j_{mn}(\mathfrak{g}_\ell)\,|\mathfrak{g}^{-1}\mathfrak{g}_\ell\rangle\,\langle\mathfrak{g}^{-1}\mathfrak{g}_\ell|\\ &= \int \mathrm{d}\mathfrak{g}_\ell\, D^j_{mn}(\mathfrak{g}\mathfrak{g}_\ell)\,|\mathfrak{g}_\ell\rangle\,\langle\mathfrak{g}_\ell| \quad \text{(replacing } \mathfrak{g}_\ell \mapsto \mathfrak{g}\mathfrak{g}_\ell \text{ and using (3.1))}\\ &= D^j_{mm'}(\mathfrak{g})\hat{U}^j_{m'n},\end{aligned} \tag{3.9}$$

where in the first line we started with (3.8), in the second line, we used (3.5) to transform the states, in the third line we used the invariance property (3.1) of the Haar measure, and in the final line we used the fact that a group representation is a homomorphism, so that $D^j_{mn}(\mathfrak{g}\mathfrak{g}_\ell) = D^j_{mm'}(\mathfrak{g})D^j_{m'n}(\mathfrak{g}_\ell)$. A similar result holds for the transformation of the link operators under right translation, so that in summary we have

$$\begin{aligned}\hat{\Theta}_{L\mathfrak{g}}\hat{U}^j_{mn}\hat{\Theta}^\dagger_{L\mathfrak{g}} &= D^j_{mm'}(\mathfrak{g})\hat{U}^j_{m'n},\\ \hat{\Theta}_{R\mathfrak{g}}\hat{U}^j_{mn}\hat{\Theta}^\dagger_{R\mathfrak{g}} &= \hat{U}^j_{mn'}D^j_{n'n}(\mathfrak{g}).\end{aligned} \tag{3.10}$$

This implies that the commutation relations between the link operators and electric operators are

$$\begin{aligned}\Big[\hat{E}^a_L, \hat{U}^j_{mn}\Big] &= T^{ja}_{mm'}\hat{U}^j_{m'n},\\ \Big[\hat{E}^a_R, \hat{U}^j_{mn}\Big] &= \hat{U}^j_{mn'}T^{ja}_{n'n},\end{aligned} \tag{3.11}$$

where the T^{ja} are the generators of the Lie group in the representation j, and there is no sum on j. (In what follows, if the representation label is omitted then we assume that the defining representation is being used.)

The left and right electric operators are related to each other by parallel transport

$$\hat{E}^a_L = \hat{U}^1_{ab}\hat{E}^b_R = \hat{E}^b_R\hat{U}^1_{ab}, \tag{3.12}$$

where the $j = 1$ representation is the adjoint one so the indices mn are replaced with group indices ab. The link operator $\hat{U}^1$ in the adjoint representation is related to the link operator in the defining representation, $\hat{U}$, according to

$$\hat{U}^1_{ab} \equiv 2\,\mathrm{Tr}(\hat{U}^\dagger T^a \hat{U} T^b). \tag{3.13}$$

From this, we can compute

$$\begin{aligned}\hat{U}^1_{ac}\hat{U}^1_{bc} &= 4\hat{U}^\dagger_{mn}T^a_{np}\hat{U}_{pq}T^c_{qm}\hat{U}^\dagger_{rs}T^b_{st}\hat{U}_{tu}T^c_{ur}\\ &= 2\left(\hat{U}^\dagger_{mn}T^a_{np}\hat{U}_{pr}\hat{U}^\dagger_{rs}T^b_{st}\hat{U}_{tm} - \frac{1}{N}\hat{U}^\dagger_{mn}T^a_{np}\hat{U}_{pm}\hat{U}^\dagger_{rs}T^b_{st}\hat{U}_{tr}\right)\\ &= 2\left(T^a_{np}T^b_{pn} - \frac{1}{N}T^a_{nn}T^b_{ss}\right)\\ &= 2\,\mathrm{Tr}(T^aT^b).\end{aligned} \tag{3.14}$$

To get from the first line to the second, we used the well-known identity satisfied by the generators of the Lie algebra of SU(N) in the defining representation,

$$T^c_{qm}T^c_{ur} = \frac{1}{2}\left(\delta_{qr}\delta_{mu} - \frac{1}{N}\delta_{qm}\delta_{ur}\right). \tag{3.15}$$

To go from the second line of (3.14) to the third, we used the unitarity of the link operator matrix $(\hat{U}^\dagger)_{nm'}\hat{U}_{m'm} = \delta_{nm}\mathbb{1}$. To go from this to the final line, we used the fact that the trace of any Lie algebra generator is zero, so that $T^a_{nn} = 0$. Thus referring to our normalisation condition (2.3) for the trace of T^aT^b, we see that the adjoint link operator is an orthogonal matrix of operators,

$$\hat{U}^1_{ac}\hat{U}^1_{bc} = \delta_{ab}\mathbb{1}. \tag{3.16}$$

Then recalling that the left and right electric operators are related by parallel transport according to (3.12), we see that their quadratic Casimirs must be equal to each other as operators,

$$\hat{E}^a_L\hat{E}^a_L = \hat{E}^b_R\hat{U}^1_{ab}\hat{U}^1_{ac}\hat{E}^c_R = \hat{E}^a_R\hat{E}^a_R \equiv \hat{E}^2. \tag{3.17}$$

We have now found a complete set of commuting electric operators, $\hat{E}^z_L$, $\hat{E}^z_R$, and $\hat{E}^2$. All states in the Hilbert space may then be written as

$$|jm_Lm_R\rangle\,, \tag{3.18}$$

where j, m_L, m_R are the quantum numbers corresponding to $\hat{E}^z_L$, $\hat{E}^z_R$, and $\hat{E}^2$, respectively. The quantum number j takes on half-integer values, while m_L and m_R each independently range from $-j$ to $+j$ in integer steps. This means that for a fixed half-integer j, there are $(2j+1)^2$ states with total 'angular momentum' j.

The overlap of these states with the group element basis states is given again by the representation matrix

$$\langle\mathfrak{g}|jm_Lm_R\rangle = \sqrt{\frac{\dim(j)}{|G|}}D^j_{m_Lm_R}(\mathfrak{g}), \tag{3.19}$$

where $\dim(j) = 2j+1$ is the dimension of the spin-j representation and $|G| = \int \mathrm{d}\mathfrak{g}$ is the volume of the group when integrated over the Haar measure; for SU(2) this is given by $|G| = 16\pi^2$. The irrep basis states are eigenstates of a maximal commuting set of the electric operators

$$\begin{aligned}
\hat{E}^2\,|jm_Lm_R\rangle &= j(j+1)\,|jm_Lm_R\rangle \\
\hat{E}^z_L\,|jm_Lm_R\rangle &= m_L\,|jm_Lm_R\rangle \\
\hat{E}^z_R\,|jm_Lm_R\rangle &= m_R\,|jm_Lm_R\rangle\,.
\end{aligned} \tag{3.20}$$

3.3 The Kogut-Susskind Hamiltonian

We are now in a position to construct the lattice Hamiltonian. On each link of the lattice, we have a copy of the one-link Hilbert space that we have developed above. Each operator is labelled by the link $\ell(n, e_i)$ to which it belongs; for example, $\hat{U}_\ell = \hat{U}(n, e_i)$. Operators belonging to different links commute with each other.

In the lattice theory, a gauge transformation that was originally taken as an independent colour rotation at every location in spacetime now becomes an independent colour rotation at each lattice site. We denote such a gauge transformation by $\Omega(n)$. Since we are working in the Weyl gauge $A_0 = 0$, our gauge transformations have no time dependence.

We note that a general gauge transformation on the whole lattice can be formed by combining individual gauge transformations which each affect only a single lattice site. We therefore let $\Omega = \Omega(n)$ be the transformation at site n. All link operators $\hat{U}(n, e_i)$ extending from site n in a positive direction are affected at their left endpoint by the gauge transformation according to (2.14). From (3.10), this can be expressed as the passive transformation

$$\hat{U}^j_{mn}(n, e_i) \mapsto D^j_{mm'}(\Omega)\hat{U}^j_{m'n} = \hat{\Theta}_{L\Omega}\hat{U}^j_{mn}\hat{\Theta}^\dagger_{L\Omega}. \tag{3.21}$$

If this is instead viewed as an active transformation made on the state of the link, we have

$$|\psi\rangle \mapsto \hat{\Theta}^{\dagger}_{L\Omega}\,|\psi\rangle\,. \tag{3.22}$$

Similarly, all link operators $\hat{U}(n-e_i,e_i)$ entering site n from a negative direction are affected at their right endpoint by the gauge transformation as

$$\hat{U}^{j}_{mn}(n-e_i,e_i) \mapsto \hat{U}^{j}_{mm'}D^{j}_{m'n}(\Omega^{-1}) = \hat{\Theta}^{\dagger}_{R\Omega}\hat{U}^{j}_{mn}\hat{\Theta}_{R\Omega}. \tag{3.23}$$

In the active picture, the states are transformed via

$$|\psi\rangle \mapsto \hat{\Theta}_{R\Omega}\,|\psi\rangle\,. \tag{3.24}$$

In what follows, we will use the active sense of the transformation.

We may now express the operator producing the gauge transformation at site n as

$$\hat{\Theta}_{\Omega}(n) = \prod_{i=1}^{d}[\hat{\Theta}_{L\Omega}(n,e_i)^{\dagger}\hat{\Theta}_{R\Omega}(n-e_i,e_i)]. \tag{3.25}$$

Such an operator can always be expressed as

$$\hat{\Theta}_{\Omega}(n) = \exp(i\phi^{a}(\Omega)\hat{G}^{a}(n)) \tag{3.26}$$

where $\phi^{a}(\Omega)$ are normal coordinates for Ω, and $\hat{G}^{a}(n)$ is the Hermitian operator which generates gauge transformations at site n. Since all operators in (3.25) commute with each other, we may use (3.6) to write

$$\begin{aligned}\hat{\Theta}_{\Omega}(n) &= \prod_{i=1}^{d}\exp\big(-i\phi^{a}(\Omega)\hat{E}^{a}_{L}(n,e_i)\big)\exp\big(i\phi^{a}(\Omega)\hat{E}^{a}_{L}(n-e_i,e_i)\big)\\ &= \exp\left(i\phi^{a}(\Omega)\sum_{i=1}^{d}\Big[\hat{E}^{a}_{R}(n-e_i,e_i)-\hat{E}^{a}_{L}(n,e_i)\Big]\right)\end{aligned} \tag{3.27}$$

and hence

$$\hat{G}^{a}(n) = \sum_{i=1}^{d}\Big[\hat{E}^{a}_{R}(n-e_i,e_i)-\hat{E}^{a}_{L}(n,e_i)\Big]. \tag{3.28}$$

This is the analogue of the covariant divergence of the chromo-electric field, D_iE^i. However, the lattice analogue of Gauss' law, $\hat{G}^{a}(n)=0$ is not true as an operator equation, and must be imposed as a constraint on the Hilbert space of states. That is, every state of the whole lattice that corresponds to a physical state $|\Psi_{\text{phys}}\rangle$ is required to satisfy the equation

$$\hat{G}^{a}(n)\,|\Psi_{\text{phys}}\rangle = 0, \tag{3.29}$$

for all sites n. Referring to the arguments above, we see that this is equivalent to the requirement that physical states are invariant under all gauge transformations,

$$\hat{\Theta}_{\Omega}(n)\,|\Psi_{\text{phys}}\rangle = |\Psi_{\text{phys}}\rangle\,, \quad \forall\,\Omega(n),\ \forall\, n. \tag{3.30}$$

We can now finally construct the lattice Hamiltonian. Switching back to the passive viewpoint, the action of a gauge transformation on the electric operators $\hat{E}_L = \hat{E}^{a}_{L}T^{a}$ and $\hat{E}_R = \hat{E}^{a}_{R}T^{a}$ and the link

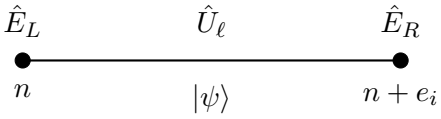

Figure 3.1: A single link of the Hilbert space, with its associated operators placed according to their gauge transformation properties. Based on a diagram from [2].

operators $\hat{U}(n, e_i)$ is

$$\hat{E}_L(n, e_i) \mapsto \Omega(n)\, \hat{E}_L(n, e_i)\, \Omega(n)^\dagger \tag{3.31}$$

$$\hat{E}_R(n, e_i) \mapsto \Omega(n + e_i)\, \hat{E}_R(n, e_i)\, \Omega(n + e_i)^\dagger \tag{3.32}$$

$$\hat{U}(n, e_i) \mapsto \Omega(n)\, \hat{U}(n, e_i)\, \Omega(n + e_i)^\dagger, \tag{3.33}$$

where $\Omega(n)$ is the gauge transformation function in the defining representation.

We first define the electric Hamiltonian of the lattice, by noting that the formulae above imply that the trace of the quadratic Casimir,

$$\operatorname{Tr} \hat{E}^2 = \frac{1}{2} \hat{E}_L^a \hat{E}_L^a = \frac{1}{2} \hat{E}_R^a \hat{E}_R^a, \tag{3.34}$$

is gauge-invariant. This allows us to define the electric Hamiltonian of the lattice by summing over every link:

$$\hat{H}_E = \frac{g^2}{2a} \sum_\ell \hat{E}_\ell^a \hat{E}_\ell^a. \tag{3.35}$$

To define the magnetic Hamiltonian of the lattice, we must work with the link operators. Consider a closed loop of links C which begins and ends at site n. We note that (3.33) implies that any ordered product of oriented link operators along C transforms as

$$\hat{U}[C] \mapsto \Omega(n) \hat{U}[C] \Omega(n)^\dagger, \tag{3.36}$$

where

$$\hat{U}[C] = \prod_{\ell \in C} (\hat{U}_\ell)^{\sigma_\ell}, \tag{3.37}$$

with $\sigma_\ell = \pm 1$ if link ℓ is traversed in the positive or negative orientations of C, respectively.

The smallest nontrivial loop on the lattice is a square consisting of four links. This is called a *plaquette*, which we will denote by p, and is described by a site n and two directions (e_i, e_j). This is illustrated in Figure 3.2. We can thus write down the most local gauge-invariant object formed from link operators:

$$\operatorname{Tr} \hat{P}_p = \operatorname{Tr} \Big[\hat{U}(n, e_i) \hat{U}(n + e_i, e_j) \hat{U}^\dagger(n + e_j, e_i) \hat{U}^\dagger(n, e_j) \Big]. \tag{3.38}$$

We can now obtain the magnetic Hamiltonian of the lattice by summing over all plaquettes:

$$\hat{H}_B = \frac{1}{2g^2 a} \sum_p \operatorname{Tr}[2I - \hat{P}_p - \hat{P}_p^\dagger], \tag{3.39}$$

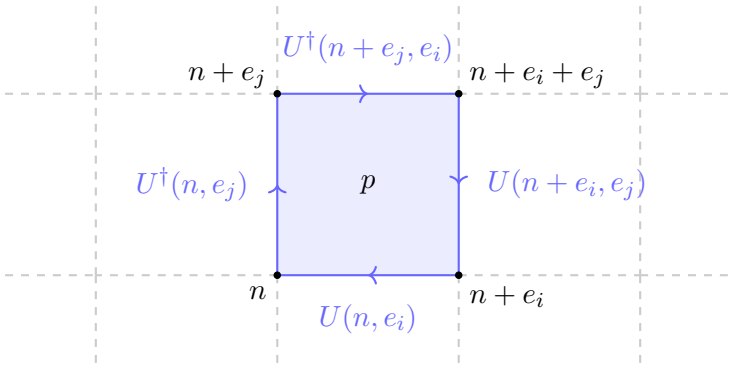

Figure 3.2: A single plaquette p, described by a site n and two directions (e_i, e_j).

where I is the 2×2 identity matrix, which has been included to ensure that $\hat{H}_B$ is positive definite. The sum is taken only over positively-oriented plaquettes, with $i < j$.

Finally, the full lattice Hamiltonian is the sum of the electric and magnetic Hamiltonians,

$$\hat{H} = \hat{H}_E + \hat{H}_B. \tag{3.40}$$

This is known as the *Kogut-Susskind Hamiltonian*, and was first introduced in [13].

4 Bases and Truncation Schemes

In order to simulate a lattice gauge theory on a classical or quantum computer, it is necessary to choose a basis in the Hilbert space to represent operators and states. Furthermore, for a bosonic variable such as a gauge field the Hilbert space at a single link is infinite-dimensional and must be truncated when performing simulations. We are thus interested in selecting a basis and corresponding truncation scheme such that the truncated theory accurately represents the continuous theory for the observables of interest. The truncated theory must also have controlled convergence properties as we increase the number of basis states.

The most common choices of bases are the electric and magnetic bases. Below, we describe these and discuss their truncation schemes.

4.1 The Electric Basis

An electric basis is a basis in which the operators $\hat{E}^2 = \hat{E}_L^2 = \hat{E}_R^2$ are diagonal. To fully specify an electric basis, we must choose which additional mutually-commuting operators are diagonal; it is most common to choose the $\hat{E}_L^z$ and $\hat{E}_R^z$ operators. The states $|jm_Lm_R\rangle$ are then used as a basis on each link of the lattice, where j denotes the eigenvalue of $\hat{E}^2$, and m_L and m_R denote the eigenvalues of $\hat{E}_L^z$ and $\hat{E}_R^z$, respectively, as in (3.20). This basis is called the *irrep basis*, and in this basis the electric Hamiltonian $\hat{H}_E$ is diagonal.

This representation works best when the electric Hamiltonian dominates. Referring to the form of $\hat{H}_E$ in (3.35), we see that the factor of g^2 means that this regime corresponds to strong coupling. In this case, the lowest-lying states are linear combinations of only the lowest-lying irreps. This means that the standard truncation scheme involves using only states with $j < j_{\max}$ for some chosen cutoff $j_{\max}$. An advantage of this representation is that the the gauge group of the truncated theory is still exactly SU(2), so that Gauss' law is exactly expressed as $\hat{G}^a(n)\,|\Psi_{\text{phys}}\rangle = 0$ for the same $\hat{G}^a$ that is defined in (3.29). This indicates that the state of the $2d$ links connected to site n must form a singlet.

The primary disadvantage of the electric basis is that it becomes inefficient at weak coupling where the magnetic Hamiltonian dominates, as can be seen from the factor of $1/g^2$ that appears in (3.39). In this regime, the magnetic Hamiltonian dominates and the lowest-lying energy eigenstates are sums of large numbers of irreps. This regime is of particular interest as we must take the weak coupling limit in order to obtain continuum physics. It is better tackled using the magnetic basis, which we now describe.

4.2 The Magnetic Basis

The magnetic basis is the group element basis already briefly described at the beginning of Section 3.2, in which the basis states are the eigenstates $|\mathfrak{g}\rangle$ of the link operators. To perform practical calculations, one generally chooses coordinates $\phi^a(\mathfrak{g})$ for the group and converts all expressions to coordinate expressions. For SU(2), the construction of the magnetic basis relies on the fact that SU(2) is diffeomorphic to the three-sphere S^3, and hence can be described by three coordinates. One obvious choice would be the Euler angles (α, β, γ), in terms of which an arbitrary matrix $U \in \mathrm{SU}(2)$ is expressed as

$$U(\alpha,\beta,\gamma) = e^{i\sigma^3\alpha/2} e^{i\sigma^2\beta/2} e^{i\sigma^3\gamma/2} = \begin{pmatrix} \cos\frac{\beta}{2} e^{i(\gamma+\alpha)/2} & \sin\frac{\beta}{2} e^{-i(\gamma-\alpha)/2} \\ -\sin\frac{\beta}{2} e^{i(\gamma-\alpha)/2} & \cos\frac{\beta}{2} e^{-i(\gamma+\alpha)/2}. \end{pmatrix} \tag{4.1}$$

The ranges of the Euler angles are

$$\alpha \in [0, 2\pi), \qquad \beta \in [0, \pi), \qquad \gamma \in [0, 4\pi). \tag{4.2}$$

Another choice of coordinates that can be used to define a magnetic basis of SU(2) are the axis-angle coordinates. As discussed above, elements of SU(2) can be represented as rotations in three-dimensional space acting on Pauli spinors. Such rotations are fully specified by an axis of rotation $\hat{n}$ and a rotation angle ω. We can parameterise the axis of rotation using spherical coordinates (θ, ϕ) as $\hat{n} = (\cos\phi\sin\theta, \sin\phi\sin\theta, \cos\theta)$. The coordinates (ω, θ, ϕ) then provide axis-angle coordinates for SU(2), and an arbitrary matrix $U \in \mathrm{SU}(2)$ can be expressed as

$$U(\omega,\theta,\phi) = e^{-i\omega\hat{n}\cdot\boldsymbol{\sigma}/2} = \begin{pmatrix} \cos\frac{\omega}{2} - i\sin\frac{\omega}{2}\cos\theta & -i\sin\frac{\omega}{2}\sin\theta e^{-i\phi} \\ -i\sin\frac{\omega}{2}\sin\theta e^{i\phi} & \cos\frac{\omega}{2} + i\sin\frac{\omega}{2}\cos\theta \end{pmatrix}. \tag{4.3}$$

The ranges of these coordinates are

$$\theta \in [0, \pi), \qquad \phi \in [0, 2\pi), \qquad \omega \in [0, 2\pi). \tag{4.4}$$

There are several ways in which the magnetic basis may be truncated, which generally involves some method of replacing the continuous group parameter $\mathfrak{g}$ with a finite sampling of points $\mathfrak{g}_i$. If one chooses the $\mathfrak{g}_i$ to form a finite subgroup of SU(2), then the resulting truncated Hilbert space maintains its group structure. An alternative choice is simply to sample some points $\mathfrak{g}_i$ which do not necessarily form a group, but which are concentrated in the support of the wavefunctions $\Psi(\mathfrak{g})$ that are to be described. The main disadvantage of this approach is the loss of group properties, particularly the loss of group composition.

4.3 Alternative Approaches

In addition to the frameworks described above, based on the Kogut-Susskind Hamiltonian and the electric and magnetic bases, there are several other methods which may be used to systematically convert an infinite-dimensional gauge theory like Yang-Mills into a finite-dimensional counterpart. Some

of these build on the Kogut-Susskind formulation considered here, while others are quite different. A short survey of the various approaches may be found in [15]. Here, we merely give a brief introduction to some of the alternative methods which could be used to encode Yang-Mills theory for quantum computation.

Prepotential and Loop-String-Hadron Formulations

Two formulations of non-Abelian lattice gauge theories which begin from the starting point of the Kogut-Susskind Hamiltonian are the *prepotential formulation* and the *loop-string-hadron formulation*. Both of these utilise the electric (irrep) basis.

In the prepotential formulation, the representation of the SU(N) link operator is broken to left and right Schwinger bosons of the SU(N) theory. These bosons are then used to build SU(N)-invariant operators at each site [15, 16].

To illustrate the prepotential approach of [16, 17], consider a single link $\hat{U}(n, e_i)$ in SU(2) lattice gauge theory. To formulate the theory on this link in terms of prepotentials, we introduce two independent doublets of bosonic creation and annihilation operators at each end of the link: $\hat{a}^\dagger_\alpha(n, e_i)$ and $\hat{b}^\dagger_\alpha(n + e_i, e_i)$, with $\alpha = 1, 2$. These are required to satisfy the commutation relations

$$[a_\alpha, a^\dagger_\beta] = \delta_{\alpha\beta}, \qquad [b_\alpha, b^\dagger_\beta] = \delta_{\alpha\beta}, \qquad [a_\alpha, a_\beta] = 0, \qquad [b_\alpha, b_\beta] = 0 \tag{4.5}$$

on every link of the lattice. Using the Schwinger boson representation of the angular momentum algebra [18], the left and right electric field operators may then be written as

$$\hat{E}^a_L(n, e_i) = \frac{1}{2} a^\dagger(n, e_i)\sigma^a a(n, e_i), \qquad \hat{E}^a_R(n, e_i) = \frac{1}{2} b^\dagger(n, e_i)\sigma^a b(n, e_i), \tag{4.6}$$

where σ^a are the Pauli sigma matrices. We also define the number operators

$$\hat{N}_a(n, e_i) = a^\dagger(n, e_i)a(n, e_i), \qquad \hat{N}_b(n, e_i) = b^\dagger(n, e_i)b(n, e_i), \tag{4.7}$$

where, on every link (n, e_i) the number of left oscillators is equal to the number of right oscillators:

$$\hat{N}_a(n, e_i) = \hat{N}_b(n + e_i, e_i) \equiv \hat{N}(n, e_i). \tag{4.8}$$

The link operator itself may then be written in the prepotential formulation as

$$\hat{U}_{\alpha\beta}(n, e_i) = \frac{1}{\sqrt{\hat{N}(n, e_i) + 1}} \Big(a^\dagger_\alpha(n, e_i) b^\dagger_\beta(n, e_i) + \tilde{a}_\alpha(n, e_i)\tilde{b}_\beta(n, e_i) \Big) \frac{1}{\sqrt{\hat{N}(n, e_i) + 1}}, \tag{4.9}$$

where we have defined $\tilde{a}_\alpha \equiv \epsilon_{\alpha\beta} a_\beta$ and $\tilde{b}_\alpha \equiv \epsilon_{\alpha\beta} b_\beta$. We see here a significant advantage of the prepotential formulation: it enables the gauge-invariant operators and states to be expressed in a local form at each site of the lattice. This removes many complications involved in expressing lattice gauge theories in terms of loops and strings [19].

The loop-string-hadron (LSH) formulation starts from the prepotential formulation, and couples the prepotential to fundamental fermions. This allows gauge-invariant bosonic and fermionic operators to be constructed; these operators are the eponymous loops, strings and hadrons. This formulation thus expresses the non-Abelian dynamics purely in terms of charge-conserving operators. Unlike in conventional lattice gauge theory where Gauss' law must be imposed as a constraint, the LSH formulation ensures that the constraints are automatic. This formulation has been developed for SU(2) gauge theory in [20], and the next aim is to extend it to SU(3) [15].

Quantum Link Models

Another approach which could potentially be used to encode gauge theories on quantum computers comes from the formulation of quantum link models (QLMs). These models were originally used in condensed matter theory, and were first introduced to particle physics via the idea of D-theory [21, 22].

In the standard Wilsonian formulation of lattice gauge theory, gauge fields are described by continuous link variables U_ℓ which live on the links between lattice sites, as we have seen above. These link variables belong to infinite-dimensional representations of the gauge group. In contrast, QLMs formulate the lattice field theory with a finite-dimensional Hilbert space. This is achieved by introducing a fictitious space dimension so that the infinite local Hilbert space can be expressed as a direct product of fixed-size Hilbert spaces on each site in the new fictitious direction. The main advantage of the QLM approach is that the Hamiltonian is local in this extended space, which may allow it to be simulated using simpler quantum circuits [15].

Quantum link models are still an area of ongoing research, and could potentially provide a new method for simulating certain theories of interest on quantum computers in the future.

Matrix Models

Matrix models of gauge theories are based on the process of dimensional reduction, in which a gauge theory may be mapped to a quantum-mechanical model while preserving some of the non-perturbative dynamics and structure of the original quantum field theory. In these models, the fundamental degrees of freedom are matrices rather than scalar or vector fields, so the Hilbert spaces are much smaller. This means that matrix models provide interesting opportunities for quantum simulations of gauge theories in the near-term, as a complement to the approaches based on truncations of lattice gauge theories described above [15]. For example, in [23] the reduction of (3+1)-dimensional SU(N) Yang-Mills theory on a small spatial torus was used to map the gauge theory to a matrix quantum-mechanical model with a calculable Hamiltonian, and the low-lying spectrum of this matrix model accurately reproduces the spectrum of the original gauge theory obtained in Euclidean lattice simulations [24].

5 Experimental Realisations

Now that we have described the theoretical basis underlying the encoding of SU(2) Yang-Mills theory on quantum computers, we are well-equipped to look at how this encoding or its variations have been implemented in experiments. Implementing non-Abelian gauge theories on quantum computers has been challenging because current quantum hardware is limited and noisy. However, significant advances in this direction have been made in recent years, as we now describe.

5.1 Quantum Simulations of U(1) Gauge Theory

Given the challenges of implementing non-Abelian gauge theories on quantum computers, it is unsurprising that the first digital qubit simulations of a lattice gauge theory focused on an Abelian case – specifically, U(1) gauge theory. These pioneering simulations were performed in [25] for U(1) with fermions in (1+1) dimensions. This work focused on the real-time evolution of the Schwinger mechanism, which involves the spontaneous creation of electron-positron pairs from the vacuum due to quantum fluctuations. This model was realised as a one-dimensional quantum field theory using a few-qubit quantum computer composed of a chain of trapped ions. Since the Schwinger model shares many important features with quantum chromodynamics, including confinement and chiral symmetry breaking, these simulations represented an important first step towards the quantum simulation of high-energy theories.

5.2 Quantum Simulations of SU(2) Yang-Mills Theory

After quantum simulations had been performed for U(1) gauge theory, the next task was to extend this approach to the real-time quantum simulation of non-Abelian lattice gauge theories, the simplest of which is SU(2) Yang-Mills theory. As this theory is the main focus of these work, we will now describe several of these quantum simulations in some detail.

SU(2) Yang-Mills on a Two-Plaquette Lattice

The first calculation in SU(2) pure gauge theory on a quantum computer was made in [26]. This utilised the electric (irrep) basis and simulated the time evolution of a one-dimensional string of two SU(2) plaquettes with periodic boundary conditions and $j_{\max} = 1/2$ on IBM's Tokyo quantum device. This was achieved through the development of an improved mapping of the angular momentum basis states, in which the local gauge symmetry was exploited to remove the angular momentum alignment variables, so that the two-plaquette system could be represented using just four qubits. The quantum circuit used for this simulation is shown in Figure 5.1.

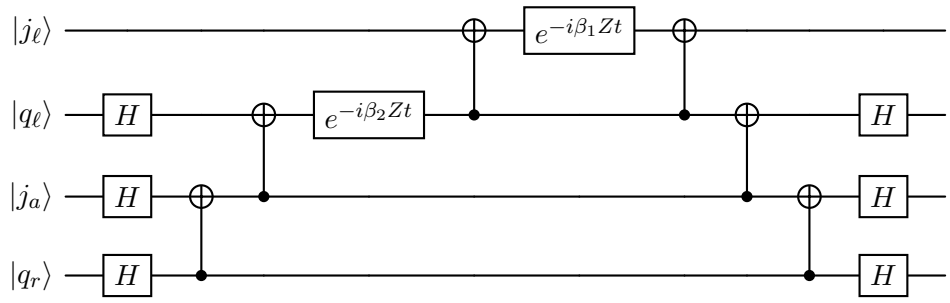

Figure 5.1: The quantum circuit used in [26] to simulate one-dimensional SU(2) gauge theory truncated to $j_{\max} = 1/2$ for a two-plaquette system with periodic boundary conditions. Here, $\beta_1 = 3/16$ and $\beta_2 = 9/16$, and $|j_\ell\rangle, |q_\ell\rangle, |j_a\rangle, |q_r\rangle$ denote the four qubits used to represent the two-plaquette system.

This circuit was used to compute the time-evolved expectation values for the electric energy contributions from the first plaquette P_1 in the two-plaquette lattice, denoted by $\langle H_{E,P_1}\rangle$, using one or two Trotter steps. The results of these computations, as drawn from [26], are shown in Figure 5.2. In this plot, the thick grey line represents the exact time evolution. The raw data for this was not provided in [26], but it was straightforward to compute (classically) in Mathematica using the expressions for the full Hamiltonian H and the first-plaquette electric Hamiltonian H_{E,P_1} which were provided in the appendix to the paper. This short calculation was carried out by defining the exact time evolution operator $U(t) = e^{-iHt}$, and repeatedly applying this to the initial state $|\psi_0\rangle$ to obtain the evolved state $|\psi(t)\rangle$ at each time step t. The desired expectation value $\langle H_{E,P_1}\rangle = \langle\psi(t)| H_{E,P_1} |\psi(t)\rangle$ was then computed at each time step using the given expression for H_{E,P_1} to produce the graph shown in Figure 5.2.

It is clear from the plot that the results obtained from the quantum computation are reasonably close to the exact values after two Trotter steps. This is because the measurement of the electric contributions are localised to the four-dimensional physical subspace, so they are well determined after only a small number of samples. In contrast, the energy contributions from the magnetic Hamiltonian are distributed throughout the Hilbert space, so measurements of the magnetic contributions would require increased sampling [26]. The results are significant as they provide a promising glimpse of how quantum computers can be used to perform calculations in SU(2) Yang-Mills theory.

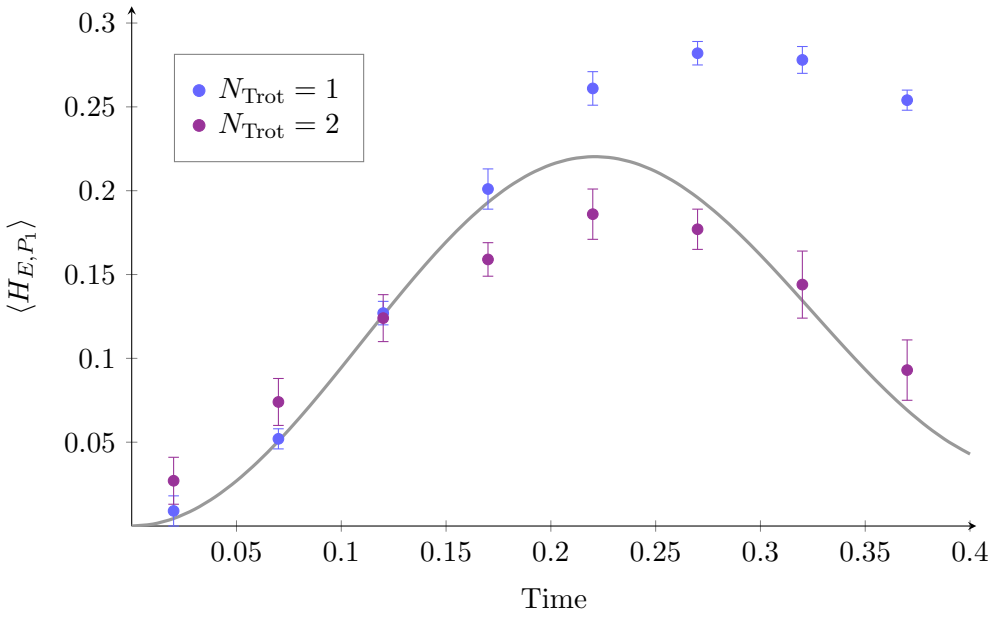

Figure 5.2: The expectation value of the contribution of the first plaquette to the electric energy, in the two-plaquette lattice with periodic boundary conditions and coupling $g^2 = 0.2$, as computed on IBM's Tokyo device in [26] using one or two Trotter steps. The thick grey line is the exact time evolution, as computed classically. The data is taken from [26].

One of the problems associated with the use of current quantum hardware is *decoherence*, which is the process by which a quantum system loses some of its properties due to interactions with its environment. This process means that states which are originally in the physical, gauge-invariant subspace may not remain in this subspace after time evolution. It is important to study the extent to which states remain in the gauge-invariant subspace on current quantum devices in order to understand the hardware limitations currently imposed on quantum simulations of lattice gauge theories. An analysis of this was carried out in [26], the results of which are shown in Figure 5.3. It was found that approximately 45% of the states with a single Trotter step ($N_{\text{Trot}} = 1$) remained in the physical subspace, while for two Trotter steps ($N_{\text{Trot}} = 2$), only approximately 25% of the states remained in the physical subspace.

This decoherence can be reduced by applying error mitigation techniques. An example of such a technique which was used in [26] is *CNOT extrapolation*. This involves inserting CNOT gates into a quantum circuit to artificially increase the error rates in a controlled manner. The circuit is run with varying numbers of these CNOT insertions to create multiple noisy datasets, and an extrapolation technique is applied to these datasets to estimate the ideal, noiseless result in the zero-error limit. When CNOT extrapolation was applied to the $N_{\text{Trot}} = 1$ case, the percentage of states remaining in the gauge-invariant space was found to increase to approximately 65%. However, CNOT extrapolation did not increase the survival population for $N_{\text{Trot}} = 2$. This is because quantum coherence is lost in a four-dimensional physical space embedded onto four qubits, so that CNOT extrapolation is no longer effective.

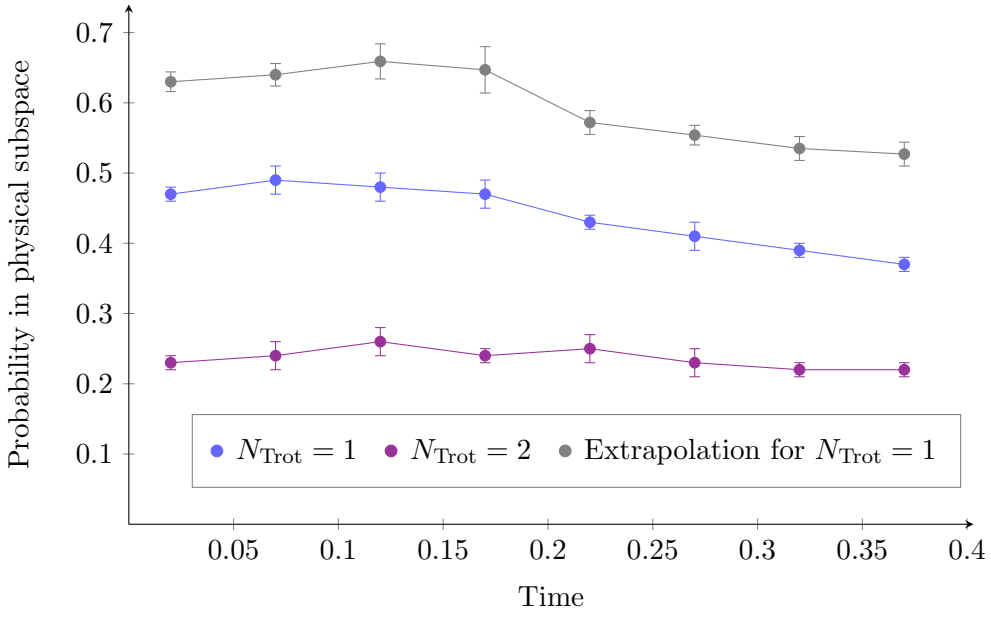

Figure 5.3: The probability of states remaining in the gauge-invariant physical subspace of the two-plaquette lattice, for simulations performed on the IBM Tokyo device using either one or two Trotter steps, along with the CNOT-extrapolated result for one Trotter step. The data is taken from [26].

SU(2) Yang-Mills on a Quantum Annealer

Another example of the simulation of SU(2) pure gauge theory on a quantum device may be found in [27], in which the theory is implemented on a quantum annealer. In classical computing, annealing is a technique used to find the minimum of a function by gradually lowering the system's temperature, which allows it to settle into a state of minimum energy. Quantum annealing serves a similar purpose, but instead of following a classical trajectory to minimise the energy, it exploits quantum tunnelling to move between different energy states.

In the paper in question, a D-Wave quantum annealer with 5760 qubits was used to implement SU(2) gauge theory for a lattice composed of a few plaquettes in a row, with periodic boundary conditions. This work goes beyond that in [26] by extending the number of plaquettes from two to four and six, and by increasing the gauge field truncation from $j_{\max}$ from 1/2 to 1 and 3/2. The simulations demonstrated that, despite the noisy qubits of existing quantum hardware, quantum annealers can produce results that are reasonably precise and accurate on lattices having only a few plaquettes.

SU(2) Yang-Mills using Self-Mitigation

The large amount of noise in current quantum devices means that the development of error mitigation techniques is a key area of research when it comes to implementing SU(2) Yang-Mills theory and other gauge theories on quantum computers. In [28], the method of *self-mitigation* was used, in which the quantum circuit is run both forwards and backwards in time. By comparing the outcomes of both of these evolutions, one can effectively identify and reduce errors arising from quantum gate imperfections and decoherence. This improved error mitigation allowed SU(2) lattice gauge theory to be simulated on a two-plaquette lattice using a circuit containing hundreds of CNOT gates. Simulations were carried out in the electric basis, with a cutoff of $j_{\max} = 1/2$. The results showed the motion of an excitation travelling across a spatial lattice in real time, a feat which would not be possible using conventional

lattice gauge theory methods on classical computers. This self-mitigation method was also used to carry out simulations on a five-plaquette lattice, and the results indicate that the method could be scaled to suit more complex lattice configurations.

5.3 Quantum Simulations of SU(3)

These recent successes in performing computations in SU(2) gauge theory on quantum devices has spurred further research into the feasibility of extending these experiments to SU(3) gauge theory in the near future. This is an important goal, because SU(3) describes the highly physically-relevant theory of quantum chromodynamics. Some of the first quantum computations in SU(3) Yang-Mills theory were performed in [29]. Recently, electric-basis calculations in SU(3) gauge theory on 5×5 and 8×8 lattices were presented in [30].

The experimental results presented here are limited to systems which are low-dimensional or small in size because of the errors that plague current quantum devices. Nevertheless, these small-scale experiments mark important progress towards the ultimate goal of using quantum computers to solve open problems in particle physics.

6 Conclusion

Yang-Mills theory is an essential building block in our modern framework of theoretical physics. While major advances have been made in simulating this theory on classical computers in the past few decades, there remain limitations and problems that mean not all systems of interest can be effectively simulated using classical devices. For this reason, there has recently been increased interest in the prospect of encoding and simulating Yang-Mills theories on quantum computers.

In this essay, we have seen how SU(2) Yang-Mills theory may be encoded for quantum computation. We began in Section 1 by introducing the concept of a lattice gauge theory, and explaining the basics of quantum computing. Section 2 provided an overview of Yang-Mills theory and its Hamiltonian formulation, while in Section 3, we saw how this Hamiltonian could be quantised and discretised to obtain the Kogut-Susskind Hamiltonian on the lattice. We then examined the electric and magnetic bases for the Hilbert space in Section 4, and discussed some of the most common truncation schemes for these bases. Finally, in Section 5, we reviewed recent efforts to implement these encoding methods on existing, noisy quantum devices.

The high noise levels present in current quantum devices impose serious constraints that hinder the full implementation of the encoding of Yang-Mills theory discussed here, particularly for the full (3+1)-dimensional theory. However, as error correction and error mitigation techniques continue to improve, it is almost certain that we will see further progress in carrying out more ambitious simulations of Yang-Mills theory on quantum computers in the future. Ultimately, leveraging quantum computing to simulate Yang-Mills theory could unlock new regimes of physics that remain inaccessible to classical methods, deepening our understanding of the fundamental forces that govern the universe.

References

[1] K. G. Wilson. 'Confinement of quarks'. *Physical Review D* 10 (8 1974), pp. 2445–2459.

[2] C. W. Bauer, I. D'Andrea, M. Freytsis and D. M. Grabowska. 'A new basis for Hamiltonian SU(2) simulations'. (2023). arXiv: 2307.11829 [hep-ph].

[3] D. Tong. *Lectures on Gauge Theory*. Lecture Notes, 2018.

[4] M. Creutz. 'Monte Carlo study of quantized SU(2) gauge theory'. *Physical Review D* 21 (8 1980), pp. 2308–2315.

[5] A. Kennedy and B. Pendleton. 'Improved heatbath method for Monte Carlo calculations in lattice gauge theories'. *Physics Letters B* 156.5 (1985), pp. 393–399.

[6] L. Funcke, T. Hartung, K. Jansen and S. Kühn. 'Review on Quantum Computing for Lattice Field Theory'. *Proceedings of Science* LATTICE2022 (2023), p. 228. arXiv: arXiv:2302.00467 [hep-lat].

[7] G. Cataldi, G. Magnifico, P. Silvi and S. Montangero. 'Simulating (2 + 1)D SU(2) Yang-Mills lattice gauge theory at finite density with tensor networks'. *Physical Reviw Research* 6 (3 2024), p. 033057. arXiv: 2307.09396 [hep-lat].

[8] A. Barenco et al. 'Elementary gates for quantum computation'. *Physical Review A* 52 (5 1995), pp. 3457–3467. arXiv: quant-ph/9503016 [quant-ph].

[9] M. A. Nielsen and I. L. Chuang. *Quantum Computation and Quantum Information*. 10th Anniversary Edition. Cambridge University Press, 2010.

[10] R. P. Feynman. 'Simulating physics with computers'. *International Journal of Theoretical Physics* 21 (6-7 1982), pp. 467–488.

[11] M. E. Peskin and D. V. Schroeder. *An Introduction to Quantum Field Theory*. Perseus Books, 1995.

[12] Y. M. Shnir. *Magnetic Monopoles*. Springer, 2005. Chap. A. Representations of SU(2).

[13] J. Kogut and L. Susskind. 'Hamiltonian formulation of Wilson's lattice gauge theories'. *Physical Review D* 11 (2 1975), pp. 395–408.

[14] T. Banks, L. Susskind and J. Kogut. 'Strong-coupling calculations of lattice gauge theories: (1+1)-dimensional exercises'. *Physical Review D* 13 (4 1976), pp. 1043–1053.

[15] C. W. Bauer et al. 'Quantum Simulation for High-Energy Physics'. *PRX Quantum* 4.2 (2023). arXiv: 2204.03381 [quant-ph].

[16] M. Mathur. 'Harmonic oscillator pre-potentials in SU(2) lattice gauge theory'. *Journal of Physics A: Mathematical and General* 38.46 (2005), p. 10015. arXiv: hep-lat/0403029 [hep-lat].

[17] M. Mathur. 'Loop approach to lattice gauge theories'. *Nuclear Physics B* 779.1–2 (2007), pp. 32–62. arXiv: hep-lat/0702007 [hep-lat].

[18] J. Schwinger. *On Angular Momentum*. Technical Report NYO-3071. U.S. Atomic Energy Commission, 1952.

[19] I. Raychowdhury and R. Anishetty. 'Prepotential Formulation of Lattice Gauge Theory'. (2014). arXiv: 1411.3068 [hep-lat].

[20] I. Raychowdhury and J. R. Stryker. 'Loop, string, and hadron dynamics in SU(2) Hamiltonian lattice gauge theories'. *Physical Review D* 101 (11 2020), p. 114502. arXiv: 1912.06133 [hep-lat].

[21] R. Brower, S. Chandrasekharan and U.-J. Wiese. 'QCD as a quantum link model'. *Physical Review D* 60 (9 1999), p. 094502. arXiv: hep-th/9704106 [hep-th].

[22] R. Brower, S. Chandrasekharan, S. Riederer and U.-J. Wiese. 'D-theory: field quantization by dimensional reduction of discrete variables'. *Nuclear Physics B* 693.1 (2004), pp. 149–175. arXiv: hep-lat/0309182 [hep-lat].

[23] M. Lüscher. 'Some analytic results concerning the mass spectrum of Yang-Mills gauge theories on a torus'. *Nuclear Physics B* 219.1 (1983), pp. 233–261.

[24] P. Van Baal. 'QCD in a Finite Volume'. *At The Frontier of Particle Physics*. World Scientific, 2001, pp. 683–760. arXiv: hep-th/0008206 [hep-th].

[25] E. Martinez, C. Muschik, P. Schindler et al. 'Real-time dynamics of lattice gauge theories with a few-qubit quantum computer'. *Nature* 534 (2016), pp. 516–519. arXiv: 1605.04570 [quant-ph].

[26] N. Klco, M. J. Savage and J. R. Stryker. 'SU(2) non-Abelian gauge field theory in one dimension on digital quantum computers'. *Physical Review D* 101 (7 2020), p. 074512. arXiv: 1908.06935 [quant-ph].

[27] S. A Rahman, R. Lewis, E. Mendicelli and S. Powell. 'SU(2) lattice gauge theory on a quantum annealer'. *Physical Review D* 104 (3 2021), p. 034501. arXiv: 2103.08661 [hep-lat].

[28] S. A Rahman, R. Lewis, E. Mendicelli and S. Powell. 'Self-mitigating Trotter circuits for SU(2) lattice gauge theory on a quantum computer'. *Physical Review D* 106 (7 2022), p. 074502. arXiv: 2205.09247 [hep-lat].

[29] A. N. Ciavarella, N. Klco and M. J. Savage. 'Trailhead for quantum simulation of SU(3) Yang-Mills lattice gauge theory in the local multiplet basis'. *Physical Review D* 103.9 (2021). arXiv: 2101.10227 [quant-ph].

[30] A. N. Ciavarella and C. W. Bauer. 'Quantum Simulation of SU(3) Lattice Yang-Mills Theory at Leading Order in Large-N_c Expansion'. *Physical Review Letters* 133 (11 2024), p. 111901. arXiv: 2402.10265 [hep-ph].